

Dietary amino acids regulate *Salmonella* colonization via microbiota-dependent mechanisms in the mouse gut

Received: 13 February 2024

Accepted: 30 April 2025

Published online: 07 May 2025



Joseph M. Pickard¹, Steffen Porwollik², Gustavo Caballero-Flores^{1,7}, Roberta Caruso¹, Shinji Fukuda^{3,4,5,6}, Tomoyoshi Soga³, Naohiro Inohara¹, Michael McClelland² & Gabriel Núñez¹✉

The gut microbiota confers host protection against pathogen colonization early after infection. Several mechanisms underlying the protection have been described, but the contributions of nutrient competition versus direct inhibition are controversial. Using an ex vivo model of *Salmonella* growth in the mouse cecum with its indigenous microbes, we find that nutrient limitation and typical inhibitory factors alone cannot prevent pathogen growth. However, the addition of certain amino acids markedly reverses the microbiota's ability to suppress pathogen growth. Enhanced *Salmonella* colonization after antibiotic treatment is ablated by exclusion of dietary protein, which requires the presence of the microbiota. Thus, dietary protein and amino acids are important regulators of colonization resistance.

The mammalian gut is colonized by trillions of individual bacteria from hundreds of species, as well as other micro-organisms, which are collectively referred to as the gut microbiota. The symbiotic relationship between the host and the gut microbiota is largely mutualistic, i.e. the microbes provide benefits to the host in exchange for a protected environment to dwell in ref. 1. Specifically, the microbiota synthesizes or liberates molecules that the host can use, and defends the space from invading bacteria². This latter function, called colonization resistance, is a complex phenomenon, but has been ascribed to a few basic mechanisms: direct actions of bacteria, including growth inhibition/killing and competition for nutrients; and indirect mechanisms, such as stimulation of the host immune system³. In a mature, healthy lower gut, many nutrients like sugars, amino acids (AAs), and respiratory electron acceptors, including O₂, are scarce due to host and microbial scavenging. It has been proposed that rather than the action of inhibitory factors, competition for one or a few key nutrients would determine the steady-state abundance of a species in the gut⁴. Indeed,

changing the nutrient landscape in the gut via diet or other methods can have a rapid and profound effect on relative bacterial abundance^{5,6}. Increased protein, fat, or sugars coming from the diet or the host can also promote the growth of pathogens or pathobionts^{7–10}. However, the critical nutrients and pathways by which the microbiota may limit pathogen colonization in the gut are incompletely understood.

The model pathogen *Salmonella enterica* subspecies *enterica* (I) serovar Typhimurium (S. Tm) is a facultative anaerobe and a metabolic generalist that can utilize many different sources of carbon (C), nitrogen (N), and energy to satisfy its growth needs^{11,12}. Nonetheless, S. Tm is normally unable to establish a productive infection when given orally to mice with a conventional microbiota¹³. It remains unclear how much of this resistance is due to host defenses, direct inhibition by bacterial metabolites^{14–16}, restriction of nutrients^{17,18}, or other yet unknown mechanisms. Here, we used a simplified ex vivo model of the cecum followed by in vivo studies to evaluate the factors governing

¹Department of Pathology and Rogel Cancer Center, University of Michigan Medical School, Ann Arbor, MI, USA. ²Department of Microbiology and Molecular Genetics, University of California, Irvine, School of Medicine, Irvine, CA, USA. ³Institute for Advanced Biosciences, Keio University, Tsuruoka, Yamagata, Japan. ⁴Gut Environmental Design Group, Kanagawa Institute of Industrial Science and Technology, Kawasaki, Kanagawa, Japan. ⁵Transborder Medical Research Center, Institute of Medicine, University of Tsukuba, Tsukuba, Ibaraki, Japan. ⁶Innovative Microbiome Therapy Research Center, Juntendo University Graduate School of Medicine, Bunkyo-ku, Tokyo, Japan. ⁷Present address: Department of Medical Microbiology and Immunology, University of Wisconsin, Madison, WI, USA. ✉e-mail: gabriel.nunez@umich.edu

initial *S. Tm* colonization of the mouse gut. We find that neither typical inhibitory factors nor nutrient competition alone can account for ex vivo growth inhibition. However, levels of AAs can modulate the microbiota's ability to resist *S. Tm*. Adding certain AAs in vivo disrupts colonization resistance, allowing *S. Tm* to grow, while AA depletion from the diet enhances resistance after antibiotic treatment. Thus, AAs are a key diet-derived determinant of colonization resistance.

Results

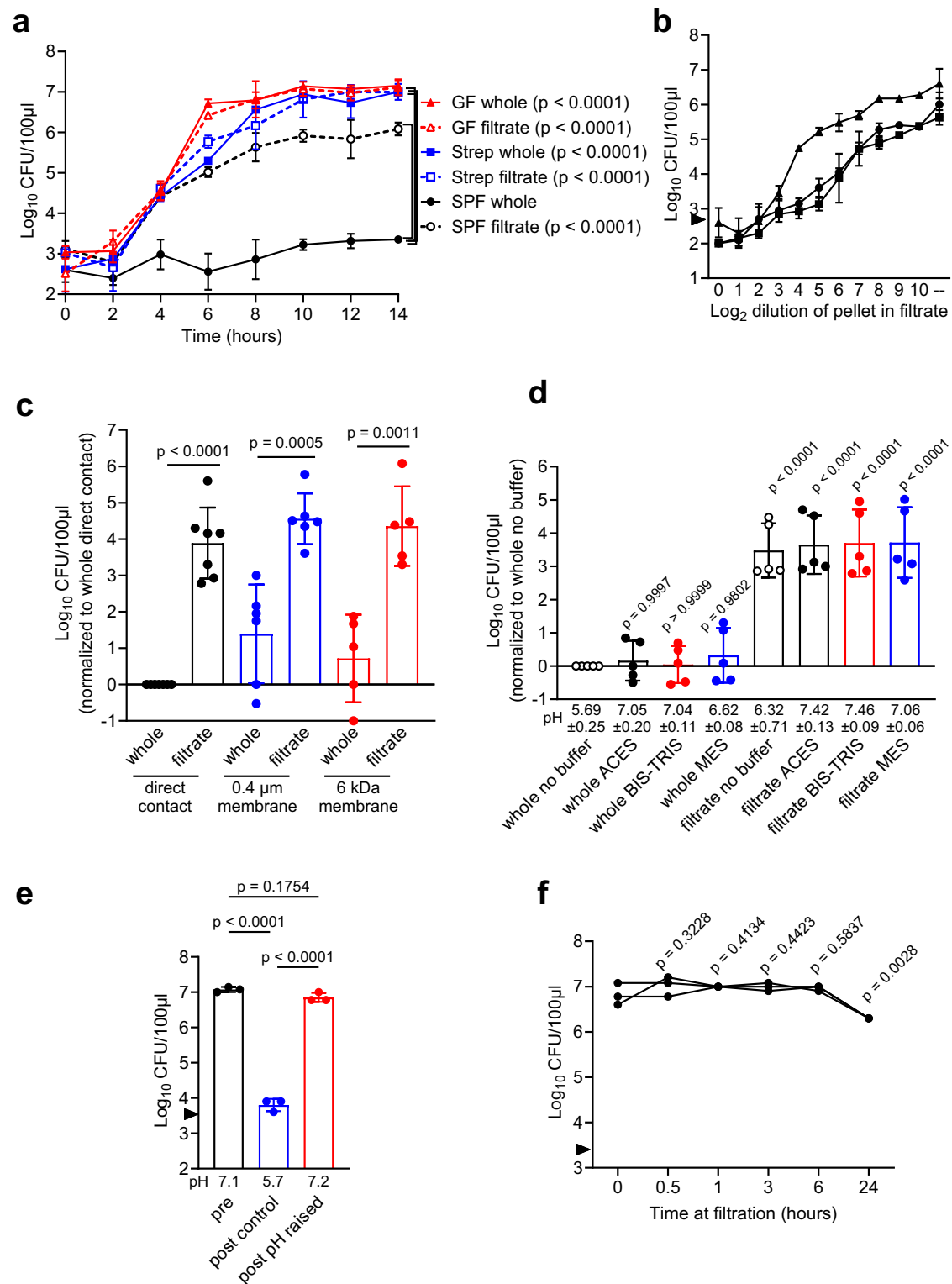
S. Tm growth is inhibited in cecal contents from specific pathogen-free mice by the continuous presence of live competitors

The cecum is the primary site of *S. Tm* replication and disease in susceptible mice¹⁹, and home to a high density and diversity of resident microbes. To investigate the mechanisms behind early colonization resistance to *S. Tm* in the mouse, we used a simple ex vivo model of *S. Tm* grown in fresh cecal contents containing the indigenous microbiota. Mouse cecal contents were removed anaerobically and homogenized in water. *S. Tm* was added to the whole or filtered homogenate, which was incubated anaerobically at 37 °C, and *S. Tm* growth was monitored by plating (Fig. 1a). This differs from similar studies in which fecal instead of cecal material was used²⁰, or cecal contents incubated for 24 h prior to adding the test bacterial strain¹⁶, which could allow microbial or metabolite abundances to change from the in vivo state. Consistent with in vivo experiments¹³ there was a significant difference in *S. Tm* growth in whole cecal contents of control specific pathogen-free (SPF) vs. streptomycin (strep)-treated SPF, or germ-free (GF) mice (all on the C57Bl/6 background). In whole SPF cecal contents, *S. Tm* was unable to replicate but remained alive, i.e. the environment was bacteriostatic (Fig. 1a). The cecal contents from most mice exhibited marked suppression of *S. Tm* growth which was relieved by filtration (Supplementary Fig. 1a). As seen in previous in vivo infections^{15,21,22}, SPF mice displayed a range of *S. Tm* suppression ex vivo and some individual mouse's cecal contents (~15%) were more permissive of *S. Tm* growth. These were excluded from further experiments as colonization resistance was not fully intact (Supplementary Fig. 1a). This variability could be due to biological variation in many factors (microbiota activity or composition, host-produced factors, amount of diet consumed), or variation in the preparation of the homogenates. When the bacteria were removed from SPF cecal homogenates by filtration or killed by heating, *S. Tm* could expand by ~3 logs, almost to the same level as in GF or strep-treated cecal material (Fig. 1a and Supplementary Fig. 1a, c). Similar results were obtained with other Gram-negative and Gram-positive bacteria, which were generally inhibited by whole cecal contents but grew well in filtrate (Supplementary Fig. 1b). Importantly, adding back pelleted material containing the live microbiota to the SPF cecal filtrate (thus keeping the filterable solutes constant) suppressed *S. Tm* growth in a dose-dependent manner (Fig. 1b). These results suggested that while some essential nutrients for *S. Tm* growth were scarce and/or soluble inhibitors were present in the SPF cecal filtrate (Fig. 1a, compare GF or strep filtrate to SPF filtrate), the presence of live competitor bacteria was necessary for complete growth suppression. Therefore, to investigate the importance of cell-cell contact with the microbiota, we separated the whole or filtered cecal contents from *S. Tm* (in the same filtrate) by a 0.4 µm or 6 kDa pore-size membrane (Fig. 1c). Growth suppression by the live microbiota was largely transmitted through the membranes, indicating that it was mediated by a small (<6 kDa) factor(s). This could be explained by continued production of an inhibitor and/or consumption of nutrients by the microbiota. Suppression through the membranes was about 1 log less effective on average than direct mixing, which could be due to cell contact-dependence²³, inefficient diffusion of molecules between the compartments, and/or the involvement of short-lived or volatile factors, such as H₂S⁴. Bubbling

the anaerobic chamber atmosphere through the whole cecal homogenate to drive off volatiles during *S. Tm* incubation had no effect on the inhibition (Supplementary Fig. 1d), and similarly, bubbling headspace gas from whole cecal homogenate through filtrate containing *S. Tm* did not suppress its growth (Supplementary Fig. 1e). Addition of excess heat-killed (HK) *S. Tm* to potentially compete with cell contact-dependent mechanisms also did not affect inhibition (Supplementary Fig. 1f, g). Together, these results suggested that neither volatile molecules nor contact-dependent inhibition played a major role in the suppression of *S. Tm* by the microbiota in this system.

Neither stable soluble inhibitors nor nutrient depletion alone mediates the suppression

We next addressed the possibility that small soluble factor(s) were actively consumed or produced by the microbiota and mediated the majority of growth suppression in our ex vivo system. Short-chain fatty acids (SCFAs) are metabolic end products produced by many gut anaerobes, and are well known to inhibit the growth of *S. Tm* and other bacteria in culture at the mM concentrations found in the cecum¹⁴. *S. Tm* can also use the SCFAs acetic, propionic and butyric acid for energy^{24,25}. Consistent with previous studies^{14,16,26}, we found that a pH of ~6 or lower is required for SCFAs to inhibit growth in culture (Supplementary Fig. 2a). The SPF mouse cecal lumen varies in measured pH, but can be at or below a pH at which SCFAs are predicted to inhibit growth¹⁴; this acidity is largely due to microbial metabolism²⁷. To assess the importance of pH and SCFAs in our model, we used three different buffers to maintain the cecal homogenate above the threshold for SCFA inhibition. Surprisingly, raising the pH did not allow *S. Tm* to grow, indicating that SCFAs and acidity were not an essential part of the inhibition in this system (Fig. 1d). Importantly, the buffers did not interfere with *S. Tm* growth when the homogenate was filtered (Fig. 1d). Next, we broadly addressed the importance of nutrient depletion or soluble inhibitors in the ex vivo system. To do this, we incubated the whole cecal homogenate (without *S. Tm*), removed samples at different timepoints, and centrifuged and filtered them. We then assessed *S. Tm*'s ability to grow in this medium. When filtrate was prepared from the cecal incubation at 16 h, *S. Tm* growth was completely inhibited (Fig. 1e). However, this inhibition was reversed by raising the acidic pH of the solution to above pH 7 (Fig. 1e). Thus, the inhibitory activity that accumulated in cecal homogenate after prolonged incubation was distinct from the immediate and continuous growth suppression, which we showed did not require acidic pH (Fig. 1d). This later pH-dependent inhibition is likely due to SCFAs produced by the anaerobic microbes during incubation of the cecal homogenate. To exclude this delayed inhibition, we repeated the cecal incubations with continuous buffering above pH 7 and collected filtrates at various times. Surprisingly, *S. Tm* grew equally well in filtrates collected at any timepoint up to 24 h (Fig. 1f). This result suggested that neither nutrient depletion nor stable, soluble inhibitory factors were responsible for the immediate growth inhibition evidenced in whole cecal homogenate. The presence of *S. Tm* was also not required to trigger an inhibitory response from the microbiota, as the same results were obtained when *S. Tm* was included in the cecal incubation (Supplementary Fig. 2b). While identifying the nature of the inhibitory factor(s) will require further work, effective suppression requires the continuous presence of the live microbiota (Supplementary Fig. 2c). Thus, the inhibition may be mediated by a very unstable factor, or one with only a temporary growth-inhibiting effect on *S. Tm*, which would require continuous replenishment to maintain its effects. The dose-dependent relationship of the cecal material to *S. Tm* final load (carrying capacity of the medium) is intriguing, as it is suggestive of nutrient limitation, although as we showed, simple nutrient depletion from the milieu cannot solely account for the inhibition in our ex vivo model of *S. Tm* growth.



Certain amino acids can counteract growth inhibition by the microbiota

All of the 20 common protein-building AAs, except for Asp and Glu, are found at lower levels in SPF mouse cecum compared to GF, suggesting that they are consumed by the gut microbiota^{10,28} (Supplementary Table 1). Many anaerobic bacteria, especially the Clostridia class that are notable for providing resistance against pathogens^{29,30}, are known to metabolize AAs as an energy source³¹. On the other hand, AAs can sometimes be detrimental to bacterial growth^{32,33}. Thus, although competition for AAs as nutrients was unlikely to cause the growth

inhibition in our model, AAs or other nutrients could still play an important role in controlling colonization resistance. We explored this by adding hydrolyzed casein protein comprising short peptides and AAs or a mixture of 20 pure L-AAs to the ex vivo cecal mixture. Surprisingly, both supplements allowed *S. Tm* to grow in the presence of the competing live bacteria and increased the final load of *S. Tm* in a dose-dependent manner (Fig. 2a). The highest concentration of AAs we added was comparable to the total amount in GF mouse cecum (Supplementary Table 1). In comparison, several monosaccharides, glycerol, or the N source NH_4Cl did not greatly improve (or were

Fig. 1 | *S. Tm* growth is inhibited in ex vivo cecum by live bacteria via small soluble factors but not nutrient depletion. **a** Cecal contents were homogenized and left whole or 0.45 μm filtered (filtrate), inoculated with *S. Tm*, incubated and sampled to determine *S. Tm* loads. Technical triplicates from $n = 1$ mouse of each treatment, representative of 2 experiments. **b** Cecal contents were homogenized and centrifuged. Supernatant was 0.45 μm filtered, and an aliquot of the pellet was resuspended and serially diluted in filtrate. CFUs were measured at 16 h (arrowhead = input). Technical replicates from $n = 3$ mice. **c** Cecal contents were homogenized, left whole or 0.45 μm filtered, and mixed directly with *S. Tm* or separated from *S. Tm* (in filtrate) by the indicated membranes. CFUs were measured as above. Material from $n = 7$ (direct contact), $n = 6$ (0.4 μm membrane), $n = 5$ (6 kDa membrane) mice or unique pools of mice. **d** Buffers were added to cecal contents and left whole or filtered. pH was measured at the end of the 16 h incubation with *S. Tm*,

and CFUs measured as above. $n = 5$ mice. **e** Cecal contents were homogenized and 0.45 μm filtered (pre) or incubated 16 h anaerobically and then filtered (post). Post-incubation filtrate was pH adjusted with NaOH or NaCl as control, and pH was measured. *S. Tm* (arrowhead = input) was grown for 16 h in the filtrates. Technical triplicates from $n = 1$ mouse cecum, representative of 3 experiments. **f** Cecal homogenates in pH 7.6 BIS-TRIS buffer were incubated anaerobically at 37 $^{\circ}\text{C}$, and an aliquot was removed and filtered at the indicated times. The filtrate was used to grow *S. Tm* (arrowhead = input) for 16 h. $n = 3$ mice. Results in **(c and d)** combined from multiple experiments. All dots or bars (except **f**) show mean \pm SD. P values are the result of one-way ANOVA with Sidák's (**a** – 14 h timepoint vs. SPF whole), Dunnett's (**d** – vs. whole no buffer, **f** – vs. time 0) or Tukey's multiple comparisons test (**e**) or unpaired two-tailed t-test (**c**). Source data are provided as a Source Data file.

detrimental to) *S. Tm* growth when added at the same concentrations (Fig. 2b). Mucic and saccharic acids and tetrathionate, which are known growth substrates in vivo^{7,12}, trended upward but did not reach significance in this experiment. To further dissect the importance of specific AAs, we focused on Arg, Asn, Gln, Gly, His, Lys, Pro, Ser, and Thr, the 9 AAs that are most strongly depleted in SPF versus GF cecum (Supplementary Table 1). We omitted Cysteine because its sensitivity to oxidation and conversion to Cystine complicates its measurement and use. A combination of the top 9 AAs were as effective as a combination of all 19 at rescuing *S. Tm* growth, while a combination of the other 10 were on average less effective (Fig. 2c), although individual mice could vary in their response. To address whether the biological activity of the AAs was important (versus a purely physical property such as charge), we compared their D and L enantiomers, excluding Gly, which is not chiral, and D-Ser which is a known growth substrate for *S. Tm* and would confound the results. Consistent with previous studies¹¹, we found that *S. Tm* does not utilize the 7 selected D-AAs as a C or N source for growth, whereas the L-forms are (Supplementary Fig. 2d). Importantly, the 7 L-AAs promoted *S. Tm* growth in the presence of the competing bacteria in the cecum, while the same AAs in their D-forms did not (Fig. 2d). Therefore, the observed growth rescue was not due to a general chemical property of the AAs but a biological function requiring the L form. Importantly, this does not distinguish whether they act directly on *S. Tm* or on the other competing microbes.

We next tested the necessity of each of the top 9 AAs for the rescue of *S. Tm* growth in the presence of live microbiota by leaving out one at a time. The results showed that none were essential (Fig. 2c), suggesting some redundancy in their functions. Next, we tested every pair of the 9 AAs for sufficiency to rescue *S. Tm* growth when added to the whole cecum. Overall, pairs containing Lys, Asn, and Ser were better at rescuing growth than pairs lacking them (Fig. 2e). The mixture of Asn, Lys, and Ser was sufficient for rescue, while the mix of Gln, Gly, and Thr was ineffective (Fig. 2f). Therefore, although there was redundancy between AAs, supplementation of specific L-AAs was sufficient to allow *S. Tm* growth in competition with the cecal microbiota.

Single amino acid catabolism by *S. Tm* plays a minor role in growth rescue

To investigate the genetic requirements for *S. Tm* to be rescued by addition of AAs in our cecal model, we performed a genetic screen with a collection of multiple-gene deletion *S. Tm* mutants (MGDs)³⁴. This collection comprised 449 mutants created by targeted lambda-red recombination, each with a segment of several genes replaced with an antibiotic resistance cassette. Collectively, these mutants delete 3476 genes, covering approximately 77% of the predicted *S. Tm* genome. Most of the multigene deletions were represented by two clones with different antibiotic markers oriented in opposite directions to reveal any difference in polarity of the resistance gene promoter on the genes adjacent to the deletion. We competed each MGD mutant against the wild-type (wt) parental strain in ex vivo cecum by adding 9 AAs and

assessed their growth by plating. The initial screen showed many MGDs that were defective in growth (Supplementary Fig. 3a). Mutants with Z-scores below 1 standard deviation from the mean (below the dotted line in Supplementary Fig. 3a) in the primary screen were tested in a second independent repetition of the experiment, and their competitive indices were calculated compared to the wt parental strain (Fig. 3a). Several of these MGDs had deleted the genes *nrdDG*, *dsbB*, and *fnr* (Fig. 3a), which are known to be generally required for anaerobic growth^{27–30}, validating the screen. Other MGDs with growth defects contained deletions in regions containing *rpe* (pentose phosphate pathway), *dksA* (stringent response), *crp* (a global transcriptional regulator), and *ppsA* (gluconeogenesis pathway). We generated specific single-gene deletions to confirm that these genes were responsible for the MGD phenotypes (Supplementary Fig. 3b). The necessity for *dksA*, *crp*, and *ppsA* led us to examine the consumption of AAs by *S. Tm* or the competing microbes in our ex vivo model.

We performed targeted metabolomics to assess the levels of free AAs in the ex vivo mixtures before and after incubation. We measured the whole cecal homogenate at time zero and compared it to whole, filtrate alone, or filtrate with wt *S. Tm* after 12 h of incubation (Fig. 3b). We subtracted the 12 h filtrate control incubation from the others to adjust for any changes that were not caused by live microbes. *S. Tm* significantly reduced the levels of 9 AAs (relative to sterile filtrate incubation), including Lys and Ser (Asn trended down but did not reach statistical significance) (Fig. 3b). Asp was also strongly depleted, in agreement with other studies^{22,35}. Whole cecal homogenate, meanwhile, produced some AAs, only significantly depleting Gln and Gly (Fig. 3b). There was no overlap in AAs consumed between the whole microbiota and *S. Tm*. Thus, although *S. Tm* consumes some AAs from the soluble milieu, it is not in direct competition with the other cecal microbes for limited AAs in this model.

Because the MGD screen identified *crp*, which primarily regulates alternative C source usage (including AA catabolism genes), and *ppsA*, which is required for growth on gluconeogenic C sources (such as AAs), we investigated whether AA catabolism by *S. Tm* could be contributing to growth in any of the ex vivo conditions. Interestingly, all of the top 9 AAs that best rescue *S. Tm* growth can be catabolized by *S. Tm*^{11,36}, compared to only 3 of the other 10 (Supplementary Table 1). In addition, the top 9 AAs can supply all C, N, and energy for *S. Tm* growing anaerobically in minimal medium, while the other 10 cannot (Supplementary Fig. 3c). We also tested the MGD mutant hits for growth in a minimal medium with glucose or AAs as the C source. 15 of 43 MGD hits had compromised growth (filled dots in Fig. 3a, Supplementary Fig. 4), indicating that they may have a defect in catabolizing AAs or glucose as C source, or could be auxotrophic for some essential molecule(s) that is absent from the minimal medium and the cecal milieu. A summary of MGD phenotypes and genotypes is found in Supplementary Table 2.

To specifically address AA catabolism genetically, we tested mutants of genes involved in the catabolism of Asn, Asp, His, Lys, Pro, Ser, and Thr, as well as the gluconeogenesis pathway gene *ppsA* and

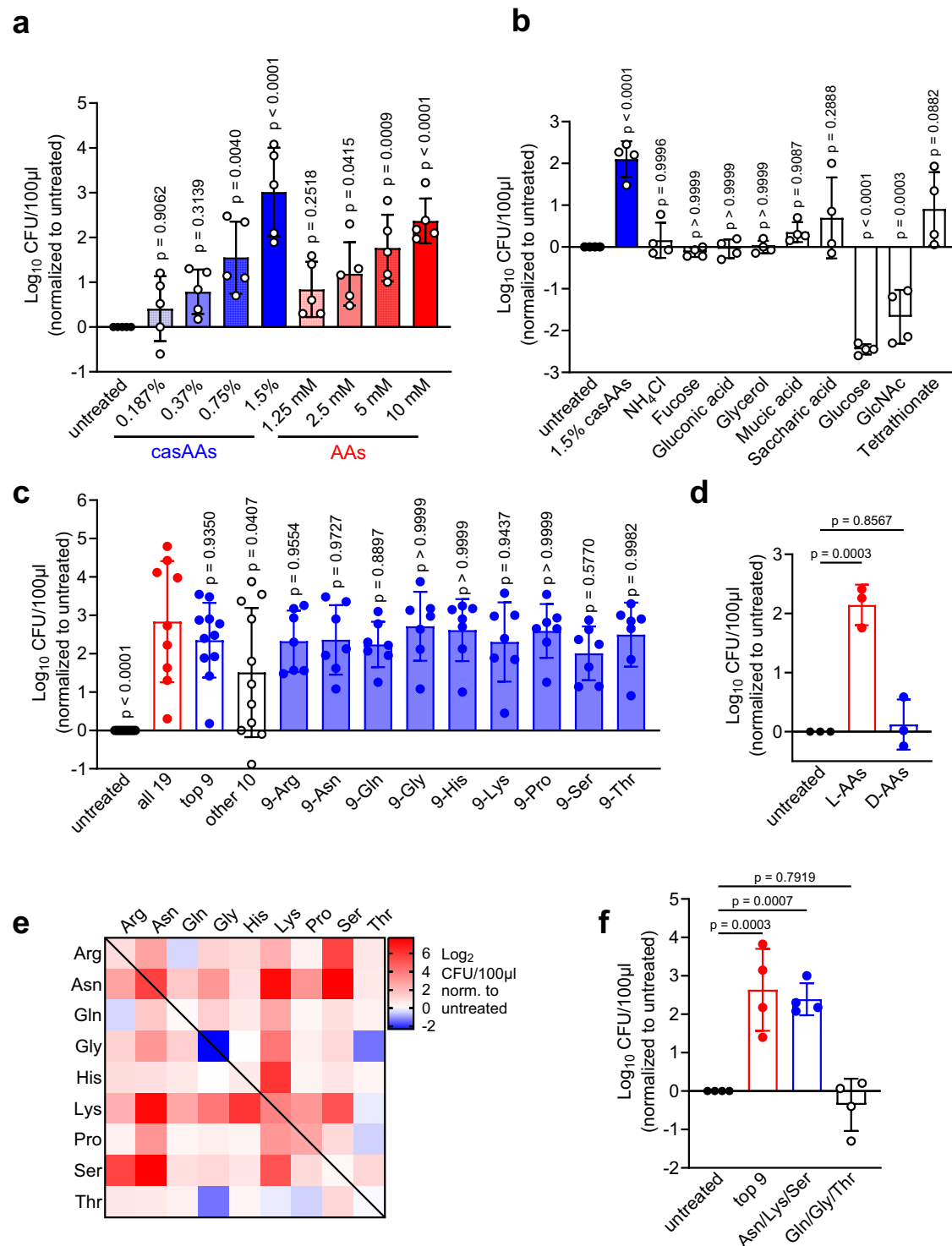
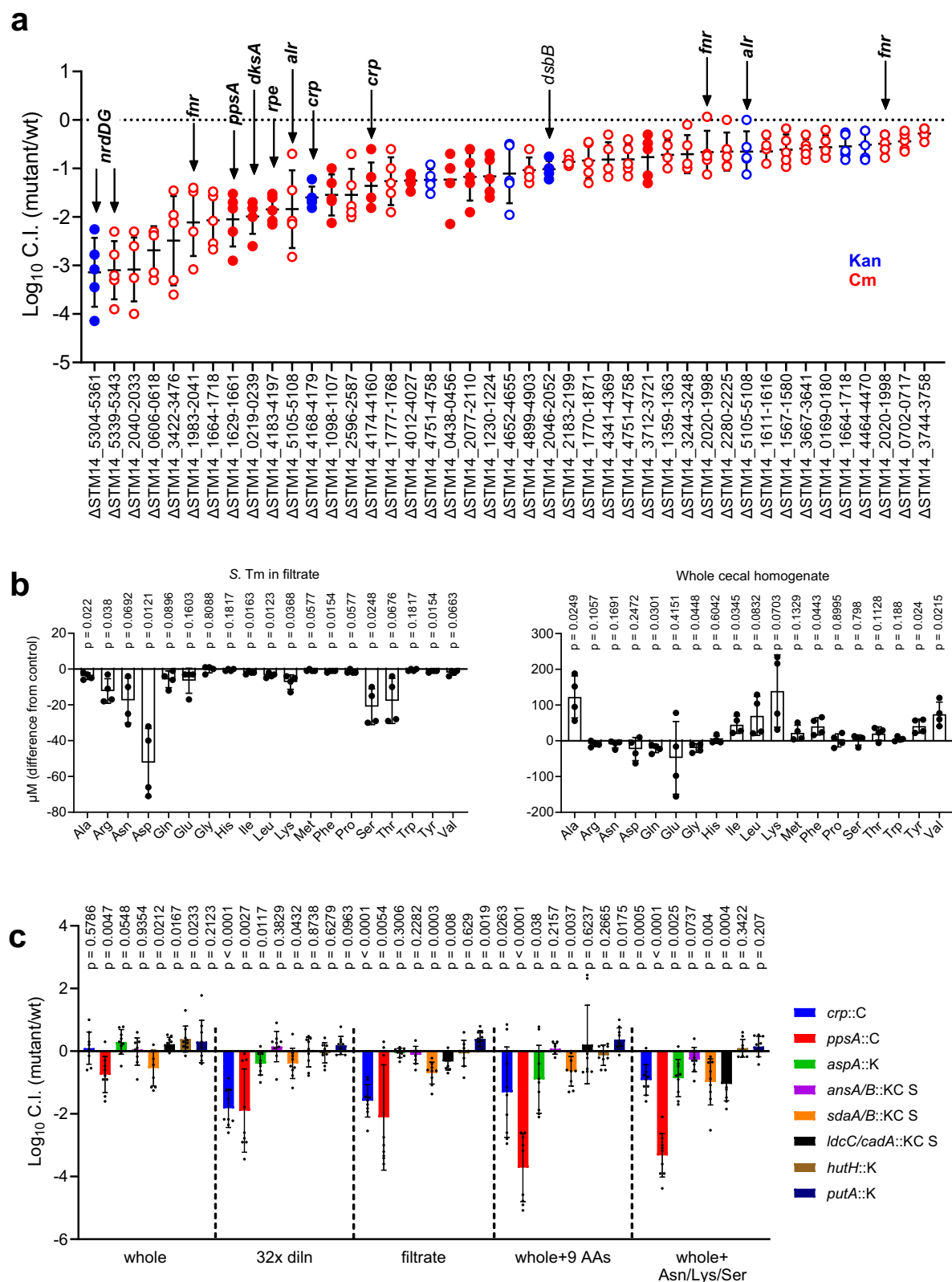


Fig. 2 | Selected amino acids can rescue *S. Tm* growth. **a** Hydrolyzed casein (casAAs) or all 20 L-AAs at the indicated final concentration of each (except Trp/Tyr at 10x less) were added to whole cecal homogenate with *S. Tm* and incubated 16 h, and CFUs counted by dilution plating. $n = 5$ mice. **b** Sugars and other chemicals were added to cecal homogenate at 10 mM (except casAAs at 1.5% w/v), *S. Tm* was added, and growth was measured as above. $n = 4$ mice. **c** Mixtures of all 19 L-AAs (-Cys), top 9, other 10, or the top 9, leaving out one at a time, were added to cecal homogenates at 10 mM each (except Trp/Tyr at 1 mM). Material from $n = 9$ (all 19), $n = 11$ (top 9), $n = 10$ (other 10), $n = 7$ (leaving out one) mice. **d** L or D enantiomers of the top 9 AAs except Gly and Ser were added to cecal homogenate at 10 mM each.

$n = 3$ mice. **e** Heat map showing *S. Tm* growth relative to untreated cecal homogenate when pairs of AAs were added at 50 mM each (except Asn at 25 mM). Single AAs (along diagonal line) are at 100 mM. Log₂ transformed mean, normalized to untreated, $n = 3$ mice. **f** The indicated AAs were added at 10 mM (top 9) or 30 mM (trios) each. $n = 4$ mice. Results combined from multiple experiments except (**b**, **d** and **e**), which are representative of 2 experiments. Bars are mean \pm SD of final CFUs normalized to untreated control. P values are the result of one-way ANOVA with Dunnett's multiple comparisons test versus untreated (except **c** - vs. all 19). Source data are provided as a Source Data file.



global carbon source regulator *crp*. These competitions were performed in conditions that permitted different amounts of *S. Tm* growth (Supplementary Fig. 3d). All pathways (except those for Lys) are CRP-regulated³⁷. As expected, the *crp* mutant had growth defects in all conditions tested (except whole cecum) (Fig. 3c). Note that it is a global regulator controlling many genes, but these include operons for catabolism of non-preferred C sources such as AAs. The *ppsA* mutant

also had a significant defect in all conditions, suggesting that gluconeogenic C sources are important in both the filtered cecal homogenate and upon addition of excess AAs. The *aspA* mutant, which is necessary for Asp catabolism and fumarate respiration (previously shown to be important for growth in the gut^{22,35}), had small defects primarily when exogenous AAs were added. Specific genes for catabolism of Asn (*ansA/B*), His (*hutH*) and Pro (*putA*) were dispensable in

Fig. 3 | Genetic and functional analysis of AA usage ex vivo. **a** Initial hits from the MGD screen (see Supplementary Fig. 3a) were tested in the same conditions, and competitive index (C.I.) was calculated by dividing mutant/wt CFUs in each well. $n = 5$ mice, mean \pm SD. Only mutants with a $p < 0.05$ by one-sample two-tailed t-test versus C.I. of 0 are shown. Arrows indicate the suspected or confirmed (bold) single-gene cause of the defect. Mutants with growth defects in minimal medium (see Supplementary Fig. 4) are indicated with filled circles. **b** Cecal homogenates were prepared from $n = 4$ mice and left whole or filtered. Filtrates with or without *S. Tm* and whole homogenates were incubated anaerobically at 37 °C. At 12 h, all samples were centrifuged, supernatants filtered, and AAs quantitated by targeted

capillary electrophoresis time-of-flight mass spectrometry (CE-TOFMS). Levels in the sterile control filtrate incubation were subtracted from each sample and mean \pm SD are shown. *P* values are the result of one-sample two-tailed t-test versus 0. **c** Cecal homogenates were left whole, diluted 32x in their own filtrate, filtered, or had 9 AAs or Asn/Lys/Ser added (as in Fig. 2f). Then the indicated mutants were grown in competition with the wt parent strain and CFUs at 16 h counted to calculate the C.I. Cecal contents from $n = 9$ mice, combined from multiple experiments. Bars are mean \pm SD. *P* values are the result of one-sample two-tailed t-test versus 0. See also Supplementary Fig. 3d. Source data are provided as a Source Data file.

all conditions (Fig. 3c). Ser catabolism genes (*sdaA/B*) had a small but significant defect in all conditions (Fig. 3c). Lys catabolism (*ldcC/cadA*, for conversion to the polyamine cadaverine) primarily became important when Lys was added (Fig. 3c). We confirmed that the phenotypes of the Asn and Ser mutants caused the expected phenotypes in culture (Supplementary Fig. 3e, f), and that the Ser and Lys mutant phenotypes were specific by restoring one of the mutated genes (*sdaA* or *cadA*) along with their endogenous promoters, which rescued growth (Supplementary Fig. 3f, g). Overall, the effect of single AA catabolism pathways was minimal and primarily occurred when excess AAs were added to the cecal homogenate, indicating that they may be used by *S. Tm* when present in large enough quantities, but are not crucial when growing in natural conditions even under some microbial competition (32x dilution condition). This could be partially explained by the redundancy between AAs (Fig. 2c) and the presence of a variety of other growth substrates.

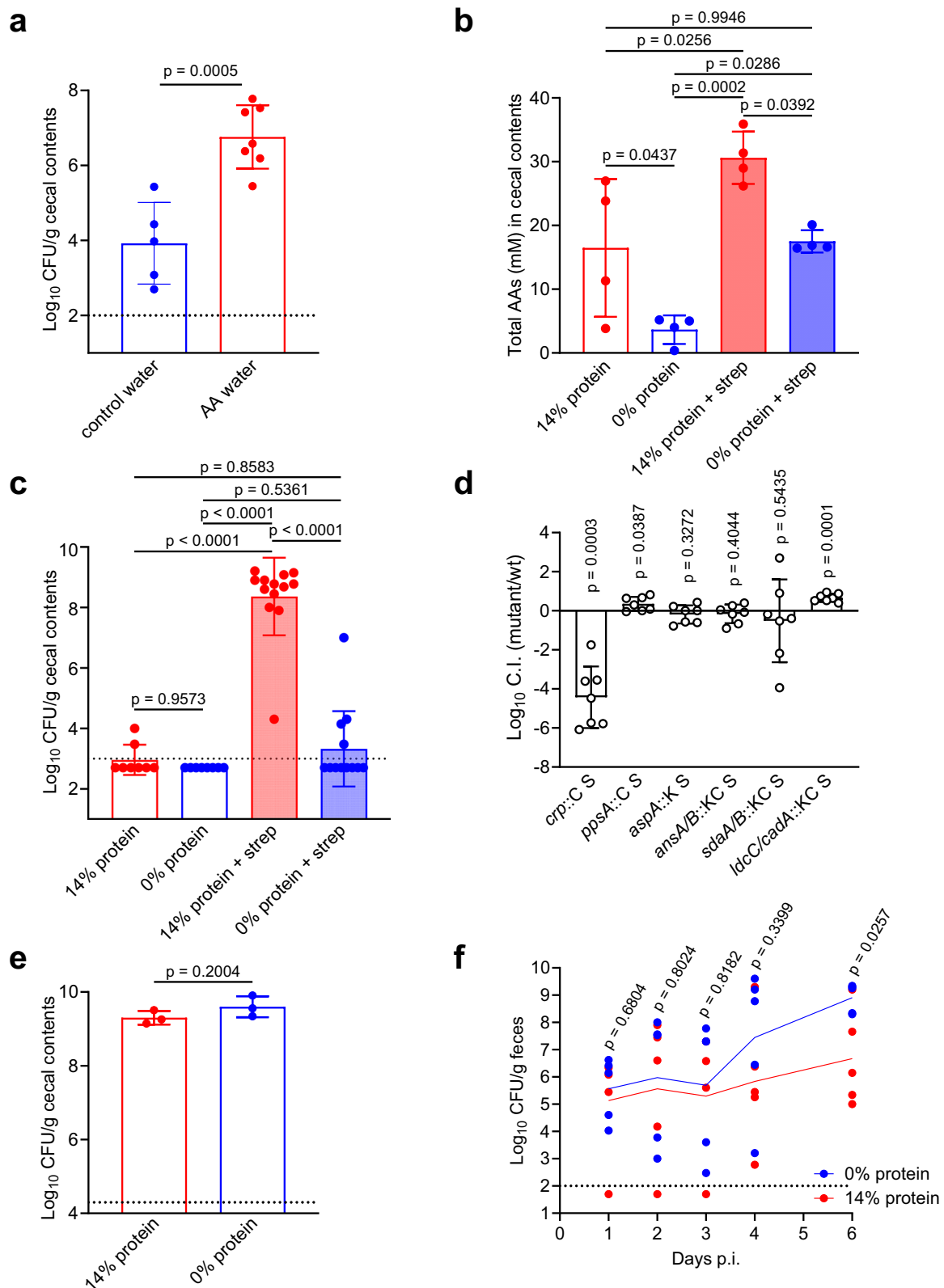
Dietary amino acids are sufficient to promote *S. Tm* colonization and essential for *S. Tm* growth rescue in the streptomycin model in vivo

A high protein diet was previously shown to promote gut colonization by another enteric pathogen, *Citrobacter rodentium*¹⁰. We tested whether specific AAs (identified in our ex vivo system) would have a similar effect on *S. Tm* infection in vivo. We provided SPF mice with drinking water containing 7 L-AAs (Arg, Asn, Gln, Lys, Pro, Ser, Thr) one day before infection with *S. Tm*, and continuing during one day of infection, after which the mice were euthanized. This short exposure to specific ingested AAs increased *S. Tm* loads in the cecum by 2–3 logs at 24 h post-infection (Fig. 4a). Water with Asn, Lys, and Ser also increased *S. Tm* loads but did not reach significance (Supplementary Fig. 5a). Thus, a short-term increase in specific ingested AAs can reduce colonization resistance and enhance the growth of *S. Tm*. Treating mice with a single gavage of the antibiotic streptomycin severely reduces colonization resistance, presumably due to killing of the protective gut bacteria¹³, and makes mice highly susceptible to *S. Tm* infection via the oral route. *S. Tm* can then expand and cause severe pathology, especially in the cecum¹⁹. To determine if strep treatment affected cecal AA levels, we performed targeted metabolomics on the cecal contents of mice that had received strep or vehicle gavage, and were placed on protein-adjusted diets. Strep-treated mice had higher amounts of total AAs in their ceca than vehicle controls (Fig. 4b, Supplementary Fig. 6a, b). To understand whether the AAs were diet-derived and were contributing to *S. Tm* expansion in this model, we compared mice fed isocaloric diets containing 0% or 14% protein. The majority of AAs in the gut lumen under normal conditions are reportedly diet-derived³⁸, thus the protein-free diet was predicted to greatly reduce the AAs available to *S. Tm* or other microbes in the gut. Indeed, mice on the protein-free diet had significantly lower levels of total AAs in their ceca than protein-fed controls (Fig. 4b). To determine whether the reduction of AAs would impact *S. Tm* colonization, mice were given strep and placed on the diets, infected one day later, and cecal loads of *S. Tm* were measured at one day post-infection (Fig. 4c). We used a strep-resistant derivative of the wt 14028S *S. Tm* strain, which retains normal virulence in strep-treated mice (Supplementary

Fig. 5b, c). Remarkably, the protein-free diet conferred almost total protection from *S. Tm* colonization (Fig. 4c), comparable to SPF mice without antibiotic treatment. Although most of the total AAs were diet-derived in untreated mice, as previously reported³⁸, there was still a significant increase in AAs in the cecal lumen upon strep treatment of the protein-free diet mice (Fig. 4b). These may have been liberated from bacteria killed by the antibiotic or produced by the host³⁵. In any case, the removal of dietary protein was able to significantly protect mice from acute *S. Tm* colonization. This was not due to faster gut transit time (Supplementary Fig. 5d). Differing from our ex vivo results, the *ppsA* and specific AA catabolism mutants of *S. Tm* did not have growth defects in the strep-treated mouse model, although the global regulator *crp* mutant did (Fig. 4d). A likely explanation is that strep treatment causes an increase in the abundance of many sugars as well as AAs, and the sugars are preferred growth substrates for *S. Tm*, thus promoting glycolysis over gluconeogenesis²¹. Therefore, because AAs could act on the microbiota rather than *S. Tm* directly, and since diet can have a strong and rapid effect on microbial abundance or activity⁶, we tested whether the protection by a protein-free diet depended on the microbiota. GF C57Bl/6 mice were placed on the two diets and infected with *S. Tm* one day later and then euthanized one day post-infection. A protein-free diet afforded no protection from *S. Tm* in the GF setting, indicating that protection by a protein-free diet against pathogen colonization was dependent on the microbiota (Fig. 4e). Interestingly, the protein-free diet also did not protect SPF mice on the CBA/J background, in which *S. Tm* colonizes the gut without antibiotic pretreatment (Fig. 4f). Collectively, these results indicate that dietary amino acids are sufficient to promote robust *S. Tm* colonization and essential for *S. Tm* growth rescue in the streptomycin model in vivo.

Discussion

We examined colonization resistance against *S. Tm* in a simplified ex vivo model, which allowed us to modify experimental conditions in ways that are not possible in mice. Surprisingly, neither inhibition by SCFAs nor competition for limiting nutrients alone played a major role in suppressing *S. Tm* growth. In our ex vivo system, the results suggest that *S. Tm* was suppressed by a small and apparently unstable factor produced by live competitor bacteria. This suppression could be negated by the addition of certain AAs. In vivo, we similarly found that adding specific AAs in the water promoted *S. Tm* colonization, while removing them from the diet caused a dramatic reduction in *S. Tm* infection. It remains unclear how dietary AAs modulate colonization resistance to *S. Tm*. Catabolism of individual AAs by *S. Tm* plays a fairly minor role in the ex vivo and in vivo (antibiotic-treated) systems. This suggests the alternative hypothesis that AAs act on particular members of the microbiota, changing their abundance, metabolic program, or production of inhibitory factors. Indeed, the protective effect of the protein-free diet disappeared in GF mice, indicating that it depends on the presence of at least some bacteria. In addition, the effect was not seen in a different mouse strain (CBA/J) that becomes colonized by *S. Tm* without antibiotic perturbation. This may mean that the protective bacteria are not present in CBA/J mice, or that antibiotics (in combination with diet manipulation) are necessary to unmask their protective ability. The cause of CBA/J susceptibility to *S. Tm* (i.e. reduced



colonization resistance) is still unclear and would benefit from further investigation. Identifying the particular bacteria necessary for protein-free diet protection (as it remains in the limited microbiota of strept-treated SPF mice but not GF) will be an important next step. It is possible that temporary dietary protein deprivation could be used to protect patients who have compromised colonization resistance due to antibiotic usage (perhaps in combination with microbiota

transplant), although total protein deprivation would need to be done with great care and for short periods only.

Mice can exhibit quite varied levels of intestinal colonization shortly after infection with model pathogens, even under extremely controlled conditions^{15,21,22}. We also observed this in our ex vivo system: ~15% of mice allowed *S. Tm* levels about 1 standard deviation above the mean and were excluded from further experimentation. Our

Fig. 4 | Dietary amino acids modulate *S. Tm* colonization. **a** SPF mice were given a mixture of 7 L-AAs (Arg, Asn, Gln, Lys, Pro, Ser, Thr) at 200 mM each in their drinking water or normal water one day prior to infection, infected with wt 14028S strep⁺ *S. Tm*, and cecal CFUs quantitated at one day post-infection. Mean \pm SD, $n = 5$ (control water) and $n = 7$ (AA water) mice, two-tailed t-test. **b** AAs were measured in cecal content supernatants from untreated or streptomycin-treated SPF mice on diets for one day, by CE-TOFMS. $n = 4$ mice, mean \pm SD, one-way ANOVA with Tukey's multiple comparisons. **c** SPF mice were treated with streptomycin and placed on 14% or 0% protein diets one day prior to infection, infected with wt 14028S strep⁺ *S. Tm*, and cecal CFUs quantitated one day post-infection. $n = 8$ (14% protein), $n = 8$ (0% protein), $n = 13$ (14% protein + strep), $n = 13$ (0% protein + strep), mean \pm SD, combined from 3 experiments, one-way ANOVA with Tukey's multiple

comparisons. **d** Streptomycin pre-treated mice on normal chow diet were infected with equal numbers of the indicated mutant strains and wt 14028S strep⁺ parent strain. Cecal contents were plated 24 h later, and C.I. was determined by dividing mutant/wt CFUs. $n = 7$, combined from multiple experiments. Bars show mean \pm SD, one-sample two-tailed t-test versus the neutral C.I. of 0. **e** GF C57BL/6 mice were placed on diets one day prior to infection, infected with wt 14028S strep⁺, and cecal CFUs quantitated one day post-infection. $n = 3$ mice, mean \pm SD, two-tailed t-test. **f** SPF CBA/J mice were placed on diets one day before infection with wt 14028S strep⁺ *S. Tm*, and feces plated to determine loads. $n = 5$ mice, line is mean, unpaired two-tailed t-test. Dotted lines are the limit of detection. Source data are provided as a Source Data file.

system could be used to take advantage of this natural variation and screen mice for ex vivo *S. Tm* growth and correlate this with the pre-existing amounts of metabolites, bacterial species, or genes in a sample from time zero. In vivo, this can only be done by sampling feces, which is an imperfect representation of conditions in the rest of the small or large intestine where *S. Tm* is attempting to colonize³⁹.

Much previous work has focused on the inhibition of bacteria like *S. Tm* by the SCFAs acetic, butyric, and propionic acids, which are produced by anaerobic gut bacteria and accumulate at millimolar concentrations in the large intestine contents^{14–16}. Although SCFAs delay bacterial growth when added to culture medium or gut material at low pH, and correlate with colonization resistance in vivo, it has been difficult to directly test their importance in situ. By controlling the pH in fresh ex vivo cecal contents, we found that SCFAs and acidity were surprisingly unnecessary for the total inhibition of *S. Tm* growth that we observed. It is a caveat that this experiment required dilution of the cecal contents in water, which reduced the concentration of inhibitors and nutrients alike. However, this unveiled a different, previously unknown mechanism of suppression. More experiments are required to address the importance of SCFAs versus other factors in colonization resistance in vivo. Interestingly, a recent study found that catabolism of Lys by *S. Tm* allowed it to better resist SCFA-induced growth inhibition in vivo in unperturbed SPF mice²⁶.

It was previously found that the mouse enteric pathogen *C. rodentium* requires AA biosynthesis genes to colonize the SPF but not the GF mouse gut¹⁰. Similar to our results, increased dietary protein promoted pathogen colonization, potentially through direct feeding of the pathogen with AAs (although a contribution of the microbiota could not be ruled out). We also found that adding AAs ex vivo or in vivo promotes *S. Tm* colonization. In addition, we observed a protective effect of protein deprivation in vivo, and this acts via the microbiota. *C. rodentium* and *S. Tm* possess the same complement of AA biosynthesis pathways, yet *C. rodentium* is much better at circumventing colonization resistance (no antibiotic pre-treatment is necessary to achieve high level colonization of SPF mice). This may be due to its specialized virulence factors, localized colonization strategy (colonic epithelial attachment), or other adaptations, which could be further explored.

Our ex vivo system allowed screening of a collection of *S. Tm* mutants, which is not feasible in vivo in normal mice due to the bottleneck imposed by colonization resistance⁴⁰. We identified several genetic loci of unclear function that could be the subject of future work and could reveal new aspects of the microbial inhibition of *S. Tm* or its growth program. This system could also be used for other medium- to high-throughput screening experiments such as screening of drug libraries for compounds that either enhance or interfere with colonization resistance.

Methods

Animals and diets

SPF mice on the C57BL/6J or CBA/J background were purchased from The Jackson Laboratory and bred under SPF conditions in our mouse

facility at the University of Michigan. GF C57BL/6 animals were also originally obtained from The Jackson Laboratory, rederived into GF conditions, and bred at the Germ-free Animal Core Facility of the University of Michigan. GF mice were bred and maintained in Techniplast cages and were monitored regularly for contamination by aerobic and anaerobic culture and Gram stains of feces/bedding to detect unculturable microbes. All mice were maintained ad lib. on the conventional rodent chow 5L0D (LabDiet), unless otherwise noted. Temperature was set at 22 °C, humidity at 30–70%, and the light/dark cycle was 12 h. Roughly equal numbers of males and females (6–10 weeks old) were used for all experiments. For in vivo experiments, mice were age-matched (less than 2 weeks difference) for each experiment, and bedding was mixed between cages 2–3 times before beginning the experiment to homogenize the gut microbiota. No sex-associated differences were observed in the reported experiments. All animal studies were approved by the University of Michigan Committee on the Care and Use of Animals.

Protein-adjusted diets from Envigo (now Inotiv) were given ad lib. and were previously used¹⁰ and are described in Supplementary Table 5.

Bacteria

All mutant *S. Tm* strains are derivatives of 14028S. Targeted mutations were created using the λ -RED recombinase system^{34,41} (further details below). Spontaneous mutants resistant to nalidixic acid or streptomycin were selected by plating 2 mL of overnight culture on LB plates with antibiotic. The plasmid conferring streptomycin resistance (pRSF1010^{SL1344}) was transferred from SL1344 to 14028S to create the 14028S Strep⁺ strain. Antibiotics were used at the following final concentrations: ampicillin 100 μ g/mL, kanamycin 50 μ g/mL, nalidixic acid 30 μ g/mL, chloramphenicol 34 μ g/mL, streptomycin 100 μ g/mL, tetracycline 15 μ g/mL.

All bacterial strains are listed in Supplementary Table 4.

Ex vivo cecal model

Mice were euthanized by isoflurane inhalation followed by cervical dislocation and removal of the cecum to a petri dish, which was immediately transferred into an anaerobic chamber (Coy Lab Products). The cecum was opened and contents were squeezed into approximately 5 volumes (2.5 mL for SPF mice, more as required for GF or strep-treated mice) of pre-reduced ultrapure water (or other solutions in water if necessary to achieve sufficient concentrations), vortexed and pipetted to homogenize. This was passed through a 100 μ m filter to remove large debris. This 2X cecal homogenate was then dispensed in 50 μ L aliquots in a 96-well round bottom plate, and 50 μ L of 2X preparations of experimental compounds or water were added for a final volume of 100 μ L per well. All experimental compounds were adjusted to pH ~6 with HCl/NaOH before use (unless otherwise noted) and pre-reduced in the chamber for at least 6 h. To separate the supernatant from pelletable material (containing live bacteria), homogenates were centrifuged for 10 min at 21,300 \times g. For titration of the pelletable material, the pellet was resuspended back to its original concentration with its own filtered supernatant, and then serially

diluted in the same filtered supernatant (excess pellet material was discarded). Cecal homogenates were heat-killed for 15 min at 80 °C. To buffer the cecal homogenates, cecal contents (2X in water) were mixed 1:1 with 200 mM ACES (adjusted to pH 6.1 or 7.5), BIS-TRIS methane (pH 5.6 or 7.6) or MES (pH 5.5 or 7.1). *S. Tm* strains were grown shaking aerobically for 6–8 h to early stationary phase in LB with appropriate antibiotics. These were centrifuged for 5 min. at 4100 × *g* and resuspended at approximately the same volume in PBS, but adjusted to equal densities according to their OD₆₀₀. These were then diluted 10⁴ times (and mixed for competition assays) in PBS to obtain a final density of ~10³ CFU per 10 µl, which was added to each well of 96-well plates containing cecal material. Plates were covered with a Breatheasy membrane (Diversified Biotech) and incubated for 16 h at 37 °C in the anaerobic chamber. A 5–20 µl aliquot was removed and serially diluted in PBS and spotted on LB plates with appropriate antibiotics for CFU counting. The bacterial inoculum (CFU per mL) was adjusted proportionately for different sized wells. For 24- or 96-well Transwells, 100 or 75 µl (respectively) of cecal filtrate with *S. Tm* was placed in the upper well and 700 or 235 µl of material (whole cecal homogenate or filtrate) in the lower well (0.4 µm pore, polycarbonate membrane, Sigma CLS3381). For dialysis tube capsules (Pur-a-lyzer mini 6000, 6–8 kDa, Sigma PURN60030), 200 µl of cecal filtrate with *S. Tm* was placed inside, and the device immersed in several mL of cecal homogenate or filtrate in a 50 mL conical tube.

For timed swapping of Transwells, *S. Tm* was incubated in filtrate in the upper wells above whole or filtered cecal homogenate in the lower wells of a 24-well Transwell plate. After 3 h of anaerobic incubation at 37 °C, the whole homogenate was removed from some lower wells, centrifuged, its supernatant filtered, and replaced (whole → filtered). The pellet from that material was resuspended in the filtrates in other lower wells (filtrate → pellet added). These were then incubated for a further 21 h. Samples from the upper wells were removed every 3 h for plating of *S. Tm* CFUs. Control wells were left continuously above filtrate or whole material.

To pass ambient atmosphere through the cecal homogenate, 1 mm outer diameter silicone tubing was inserted through a hole in the cap of a screw top 2 ml tube to reach the bottom of the tube. The tubing was sealed in place with silicone caulking. Several holes were punched in the cap with a needle to allow gas to escape. The silicone tubing was connected to a peristaltic pump (Atto Corporation) and the entire apparatus placed in the anaerobic chamber. Cecal homogenate or filtrate and *S. Tm* were added to the tube and incubated at 37 °C while chamber atmosphere was pumped through the silicone tubing to bubble through the contents at a rate of 1–2 mL/min. To pass cecal homogenate headspace gas through filtrate, an additional screw top tube was added with input and output silicone tubes inserted through the cap. Atmosphere was bubbled through the cecal homogenate in tube 1, and the output tubing carried excess gas to tube 2 where it bubbled through filtrate containing *S. Tm*.

The pH was measured with a Mettler Toledo LE422 micro pH electrode connected to a Fisher Scientific Accumet AE150 meter.

Heat-killing of *S. Tm* was done in a water bath at 65 °C for 30 min. The cells remained largely intact (distinct membrane and nucleic acid staining) upon microscopic examination. An aliquot of heat-killed bacteria originally containing ~10⁸ cells was plated on LB agar and added to liquid LB and grown for 24 h at 37 °C, which resulted in no visible growth in either condition.

Fluorescence microscopy

To verify the intactness of cells after heat-killing, heat-killed or control *S. Tm* were pelleted by centrifugation and resuspended in the same volume of PBS (~10⁹ cells/mL). The following dyes were added and cells incubated at RT for 20 min in the dark: DAPI (2 µg/mL), DiBAC4 (1 µg/mL), MM 4–64 (10 µg/mL). Cells were centrifuged again and the pellet resuspended in the residual supernatant (10 µl). 4 µl of this was placed

on a slide and coverslipped for immediate imaging on a Nikon Xi Yokogawa spinning disk confocal microscope at the University of Michigan Light Microscopy Core Facility.

Genetic screen of *Salmonella* mutants

The collection of *S. Tm* MGD mutants has been reported²⁸. For the MGD screen, mutants were spotted on 150 mm LB plates from their frozen sucrose stocks in 96-well plates. A 12-tip multichannel pipettor was used to seed 96-well round bottom plates containing 100 µl LB with appropriate antibiotics, and these were grown for 8 h at 37 °C without shaking. Cultures were checked for growth by OD₆₀₀, diluted 10⁴ times in PBS, and 5 µl were added to 50 µl 1X cecal homogenate containing 9 AAs (10 mM each). MGDs with the Kan and Cm cassette were combined in each well along with an equal amount of streptomycin-resistant wt strain as competitor. After 16 h incubation, CFUs were counted by spot dilution plating on LB with appropriate antibiotics. Z-scores for each mutant were calculated by the formula $z = (x - \mu) / \sigma$ where x is the raw CFUs, μ is the mean, and σ is the standard deviation.

Mouse infections

S. Tm strains were grown overnight in LB with appropriate antibiotics, shaking aerobically at 37 °C, then diluted 1:50 in fresh LB and shaken for 2.5 h. These cultures were centrifuged and resuspended in approximately one volume PBS but adjusted to equal densities according to their OD₆₀₀. For competitions, strains were mixed at equal ratios and diluted in PBS before gavage of 100 µl to recipient mice, giving a total dose of ~100–1000 CFUs. CBA/J mice were gavaged with ~10⁶ CFUs, after one day on protein-adjusted diets. For the streptomycin pre-treatment model, mice were gavaged with 20 mg streptomycin in 100 µl water 24 h before infection. For diet experiments, mice were moved to a fresh cage and switched to the protein-adjusted diets and gavaged with streptomycin. 24 h later they were infected with ~10–100 CFUs of *S. Tm* in 100 µl PBS. GF mice were given ~10–100 CFUs in 100 µl PBS. AAs were dissolved in deionized water at 200 mM each and 0.2 µm filter sterilized and provided to mice ad libitum as their source of drinking water.

Gut transit time measurement

1% methylcellulose was dissolved with heating to 60 °C in 0.9% saline solution, and 5% w/v Evans blue dye added. 100 µl was gavaged to mice and they were single-housed and observed until a blue fecal pellet was passed.

Construction of *S. Tm* mutant strains

Deletion mutants were generated by allelic replacement of the target genes with an antibiotic resistance cassette as previously described^{34,41}. Briefly, deletion cassettes were amplified by PCR with specific primer pairs (Supplementary Table 3) using the plasmid pKD3 (Cm^r) or pKD4 (Kan^r) as a template and including 45 bp of homology adjacent to the target region at their 5' ends. The resulting PCR products were purified by phenol/chloroform extraction and ethanol precipitation and resuspended in 15 µl water. Overnight cultures of the recipient strain containing the pKD46 (λ-RED recombinase) plasmid were diluted 1:50 in 5 mL fresh LB and induced with 0.1 M L-arabinose for 2.5 h at 30 °C, then washed repeatedly with ultrapure water, concentrated 100 times, and transformed with the purified PCR product using a MicroPulser Electroporator (BioRad). They were recovered for 1 h in 1 mL SOC medium shaking at 37 °C, incubated overnight at RT, then plated on the appropriate selective LB agar plates. Correct insertion was verified by PCR with a forward primer upstream of the replacement site and a reverse primer inside the antibiotic resistance cassette. Antibiotic resistance cassettes were removed via flip recombinase by transforming with the pCP20 plasmid and verified by spotting on appropriate antibiotic plates to check sensitivity.

Mutations were transferred to different strains using the P22 phage system (kindly provided by Dr. Manuela Raffatellu, University of California, San Diego). Briefly, donor strains were grown overnight in LB, then 200 μ L was added to 1 mL of P22 broth (containing P22 HT 105/1 int-201 lysate in LB with 0.2% glucose). This was shaken for at least 8 h at 37 °C, then centrifuged. 5 drops of chloroform were added to the supernatant, mixed to sterilize, and stored at 4 °C. To transfer mutations, recipient strains were grown overnight, and 20 μ L of lysate was added to 200 μ L recipient cultures, incubated for 15 min at RT, then 1 mL LB was added and shaken for 1 h at 37 °C. This was plated on the appropriate selective plates. Recipient colonies were then streaked on Evans blue/uranine agar to select white colonies for further use.

Complementation of mutants

The *sdaA* and *cadBA* coding regions and upstream promoter regions were amplified and inserted into the chromosome at a neutral site using an established Tn7 transposon-based system as described⁴². Briefly, the genes of interest were amplified (primers listed in Supplementary Table 3) and inserted into plasmid pGRG25. The construct was electroporated into recipient cells and grown on LB agar with ampicillin at 30°. One colony was picked and grown in liquid LB containing 1 mM L-arabinose overnight at 30°. This culture was streaked on LB agar and grown at 42° to facilitate plasmid loss. Colonies were picked and correct insertions were verified by PCR amplification and sequencing using primers on either side of the insertion site, and by functional restoration of growth on Ser for the *sdaA* complementation. Plasmid loss was confirmed by ampicillin susceptibility.

Bacterial growth curves

Strains were grown overnight with shaking in LB with appropriate antibiotics. For LB growth with SCFAs, cells were centrifuged and diluted 1:100 in anaerobic LB with 100 mM ACES, and with or without SCFAs, that was pre-adjusted to the indicated pH. The maximum 1X concentration of SCFAs was 50 mM acetic acid, 10 mM propionic acid and 25 mM butyric acid. For C/N source determinations, cells were centrifuged and washed once with Milli-Q water, resuspended in water and diluted 1:50 in anaerobic 2X M9 salts (with or without NH₄Cl) supplemented with 4 mM MgSO₄, 200 μ M CaCl₂, and 2 μ M FeSO₄. 100 μ L was added to 100 μ L of 2X nutrient sources in 96-well flat bottom plates (Corning Costar) and absorbance at 600 nm monitored every 15 min in a plate reader (BioTek Epoch 2) in an anaerobic chamber (Coy Lab Products) heated to 37 °C. 40 mM sodium nitrate was added to facilitate growth on single AAs as C sources (at 10 mM), or glucose was used at 10 mM.

Measurement of metabolite concentrations in the gut

Intestinal contents from mice or ex vivo incubations were centrifuged (17,000 \times g for 10 min) and the supernatant removed, and volume measured. Water was added to reach 200 μ L and the sample frozen at -80 °C until use. 50 μ L of sample solutions were mixed with 450 μ L of methanol containing 20 μ M each of internal standard: methionine sulfone and D-camphor-10-sulfonic acid. 200 μ L of Milli-Q water and 500 μ L of chloroform were added to the mixtures and samples were shaken. Samples were centrifuged (4600 \times g/15 min, 4 °C), supernatants were concentrated at 40 °C using a 5 kDa cutoff centrifugal filter and pellets reconstituted with 40 μ L of Milli-Q water. Metabolites were analyzed using capillary electrophoresis-time-of-flight mass spectrometry (CE-TOFMS) in both positive and negative modes using a CE capillary electrophoresis system (Agilent Technologies). Peak annotation and quantification were performed using an in-house software (MasterHands)^{43,44}. Concentrations were adjusted by the original dilution factor.

Statistics & reproducibility

Statistical analyses were performed using GraphPad Prism software version 10.4.1 (GraphPad Software Inc). CFU and C.I. data were log₁₀ transformed and then assumed to be normally distributed. Samples that fell below the limit of detection (l.o.d.) were set to half the l.o.d. Statistical tests, sample sizes and replicates are detailed in the figure legends. No statistical method was used to predetermine sample size. Mouse materials were excluded from ex vivo experiments as described in Supplementary Fig. 1a. Otherwise, no data were excluded from the analyses. The experiments were not randomized. The Investigators were not blinded to allocation during experiments and outcome assessment.

Reporting summary

Further information on research design is available in the Nature Portfolio Reporting Summary linked to this article.

Data availability

The metabolomics data generated in this study have been deposited in the DDBJ metabobank database under accession code MTBKS232 [<https://ddbj.nig.ac.jp/public/metabobank/study/>]. Source data are provided with this paper.

References

- Backhed, F., Ley, R. E., Sonnenburg, J. L., Peterson, D. A. & Gordon, J. I. Host-bacterial mutualism in the human intestine. *Science* **307**, 1915–1920 (2005).
- Pickard, J. M. & Nunez, G. Pathogen colonization resistance in the gut and its manipulation for improved health. *Am. J. Pathol.* **189**, 1300–1310 (2019).
- Caballero-Flores, G., Pickard, J. M. & Nunez, G. Microbiota-mediated colonization resistance: mechanisms and regulation. *Nat. Rev. Microbiol.* <https://doi.org/10.1038/s41579-022-00833-7> (2022).
- Freter, R., Brickner, H., Botney, M., Cleven, D. & Aranki, A. Mechanisms that control bacterial populations in continuous-flow culture models of mouse large intestinal flora. *Infect. Immun.* **39**, 676–685 (1983).
- Turnbaugh, P. J., Backhed, F., Fulton, L. & Gordon, J. I. Diet-induced obesity is linked to marked but reversible alterations in the mouse distal gut microbiome. *Cell Host Microbe* **3**, 213–223 (2008).
- David, L. A. et al. Diet rapidly and reproducibly alters the human gut microbiome. *Nature* **505**, 559–563 (2014).
- Faber, F. et al. Host-mediated sugar oxidation promotes post-antibiotic pathogen expansion. *Nature* **534**, 697–699 (2016).
- Ng, K. M. et al. Microbiota-liberated host sugars facilitate post-antibiotic expansion of enteric pathogens. *Nature* **502**, 96–99 (2013).
- Devkota, S. et al. Dietary-fat-induced taurocholic acid promotes pathobiont expansion and colitis in IL10^{-/-} mice. *Nature* **487**, 104–108 (2012).
- Caballero-Flores, G., Pickard, J. M., Fukuda, S., Inohara, N. & Núñez, G. An enteric pathogen subverts colonization resistance by evading competition for amino acids in the gut. *Cell Host Microbe* **28**, 526–533.e525 (2020).
- Gutnick, D., Calvo, J. M., Klopotoski, T. & Ames, B. N. Compounds which serve as the sole source of carbon or nitrogen for *Salmonella typhimurium* LT-2. *J. Bacteriol.* **100**, 215–219 (1969).
- Winter, S. E. et al. Gut inflammation provides a respiratory electron acceptor for *Salmonella*. *Nature* **467**, 426–429 (2010).
- Bohnhoff, M. & Miller, C. P. Enhanced susceptibility to *Salmonella* infection in streptomycin-treated mice*. *J. Infect. Dis.* **111**, 117–127 (1962).
- Bohnhoff, M., Miller, C. P. & Martin, W. R. Resistance of the mouse's intestinal tract to experimental salmonella infection. *J. Exp. Med.* **120**, 805–816 (1964).

15. Jacobson, A. et al. A gut commensal-produced metabolite mediates colonization resistance to *Salmonella* infection. *Cell Host Microbe* **24**, 296–307.e297 (2018).
16. Sorbara, M. T. et al. Inhibiting antibiotic-resistant Enterobacteriaceae by microbiota-mediated intracellular acidification. *J. Exp. Med.* **216**, 84–98 (2018).
17. Maltby, R., Leatham-Jensen, M. P., Gibson, T., Cohen, P. S. & Conway, T. Nutritional basis for colonization resistance by human commensal *Escherichia coli* strains HS and Nissle 1917 against *E. coli* O157:H7 in the mouse intestine. *PLOS ONE* **8**, e53957 (2013).
18. Eberl, C. et al. *E. coli* enhance colonization resistance against *Salmonella* Typhimurium by competing for galactitol, a context-dependent limiting carbon source. *Cell Host Microbe* **29**, 1680–1692.e1687 (2021).
19. Barthel, M. et al. Pretreatment of mice with streptomycin provides a *Salmonella enterica* serovar Typhimurium colitis model that allows analysis of both pathogen and host. *Infect. Immun.* **71**, 2839–2858 (2003).
20. Velazquez, E. M. et al. Endogenous Enterobacteriaceae underlie variation in susceptibility to *Salmonella* infection. *Nat. Microbiol.* **4**, 1057–1064 (2019).
21. Nguyen, B. D. et al. *Salmonella* Typhimurium screen identifies shifts in mixed-acid fermentation during gut colonization. *Cell Host Microbe*. <https://doi.org/10.1016/j.chom.2024.08.015> (2024).
22. Nguyen, B. D. et al. Import of Aspartate and Malate by DcuABC Drives H₂/Fumarate Respiration to Promote Initial *Salmonella* Gut-Lumen Colonization in Mice. *Cell Host Microbe* **27**, 922–936.e926 (2020).
23. Hayes, C. S., Koskineemi, S., Ruhe, Z. C., Poole, S. J. & Low, D. A. Mechanisms and Biological Roles of Contact-Dependent Growth Inhibition Systems. *Cold Spring Harb. Perspect. Med.* **4**, a010025 (2014).
24. Shelton, C. D. et al. *Salmonella enterica* serovar Typhimurium uses anaerobic respiration to overcome propionate-mediated colonization resistance. *Cell Rep.* **38**, <https://doi.org/10.1016/j.celrep.2021.110180> (2022).
25. Bronner, D. N. et al. Genetic ablation of butyrate utilization attenuates gastrointestinal salmonella disease. *Cell Host Microbe* **23**, 266–273.e264 (2018).
26. Radlinski, L. C. et al. *Salmonella* virulence factors induce amino acid malabsorption in the ileum to promote ecosystem invasion of the large intestine. *Proc. Natl Acad. Sci. USA* **121**, e2417232121 (2024).
27. Maier, B. R., Onderdonk, A. B., Baskett, R. C. & Hentges, D. J. Shigella, indigenous flora interactions in mice. *Am. J. Clin. Nutr.* **25**, 1433–1440 (1972).
28. Li, T. T. et al. Microbiota metabolism of intestinal amino acids impacts host nutrient homeostasis and physiology. *Cell Host Microbe* **32**, 661–675.e610 (2024).
29. Kim, Y.-G. et al. Neonatal acquisition of Clostridia species protects against colonization by bacterial pathogens. *Science* **356**, 315–319 (2017).
30. Rivera-Chavez, F. et al. Depletion of butyrate-producing clostridia from the gut microbiota drives an aerobic luminal expansion of salmonella. *Cell Host Microbe* **19**, 443–454 (2016).
31. Barker, H. A. Amino acid degradation by anaerobic bacteria. *Annu. Rev. Biochem.* **50**, 23–40 (1981).
32. Kajikawa, H., Mitsumori, M. & Ohmomo, S. Stimulatory and inhibitory effects of protein amino acids on growth rate and efficiency of mixed ruminal bacteria. *J. Dairy Sci.* **85**, 2015–2022 (2002).
33. Leavitt, R. I. & Umbarger, H. E. Isoleucine and valine metabolism in *Escherichia coli*. XI. Valine inhibition of the growth of *Escherichia coli* strain K-12. *J. Bacteriol.* **83**, 624–630 (1962).
34. Porwollik, S. et al. Defined single-gene and multi-gene deletion mutant collections in *Salmonella enterica* sv Typhimurium. *PLOS ONE* **9**, e99820 (2014).
35. Yoo, W. et al. *Salmonella* Typhimurium expansion in the inflamed murine gut is dependent on aspartate derived from ROS-mediated microbiota lysis. *Cell Host Microbe* **32**, 887–899.e886 (2024).
36. McClelland, M. et al. Complete genome sequence of *Salmonella enterica* serovar Typhimurium LT2. *Nature* **413**, 852–856 (2001).
37. Tierrafria, V. H. et al. RegulonDB 11.0: Comprehensive high-throughput datasets on transcriptional regulation in *Escherichia coli* K-12. *Microb. Genom.* **8**, <https://doi.org/10.1099/mgen.0.000833> (2022).
38. Kitamoto, S. et al. Dietary L-serine confers a competitive fitness advantage to Enterobacteriaceae in the inflamed gut. *Nat. Microbiol.* **5**, 116–125 (2020).
39. Levitan, O. et al. The gut microbiome—Does stool represent right? *Heliyon* **9**, e13602 (2023).
40. Maier, L. et al. Microbiota-derived hydrogen fuels *Salmonella* typhimurium invasion of the gut ecosystem. *Cell Host Microbe* **14**, 641–651 (2013).
41. Datsenko, K. A. & Wanner, B. L. One-step inactivation of chromosomal genes in *Escherichia coli* K-12 using PCR products. *Proc. Natl Acad. Sci. USA* **97**, 6640–6645 (2000).
42. McKenzie, G. J. & Craig, N. L. Fast, easy and efficient: site-specific insertion of transgenes into enterobacterial chromosomes using Tn7 without need for selection of the insertion event. *BMC Microbiol.* **6**, 39 (2006).
43. Sugimoto, M., Wong, D. T., Hirayama, A., Soga, T. & Tomita, M. Capillary electrophoresis mass spectrometry-based saliva metabolomics identified oral, breast and pancreatic cancer-specific profiles. *Metabolomics* **6**, 78–95 (2010).
44. Yamamoto, Y. et al. A Metabolomic-Based Evaluation of the Role of Commensal Microbiota throughout the Gastrointestinal Tract in Mice. *Microorganisms* **6**, <https://doi.org/10.3390/microorganisms6040101> (2018).

Acknowledgements

The authors thank Weiping Chu for expert technical assistance; the staff of the University of Michigan ULAM germ-free mouse facility; Lisa Haynes, Caitlin Reynolds, Kelsey Martin, and Amr Aboud for animal husbandry; Edward Kabara, Kelly Carnahan, Tailor Mathes and Peter Kuffa for lab management support; Jill Hakim and Jibraan Rashid for help with experiments; past and present members of the Núñez lab; Alexander Chervonsky, Tatyana Golovkina and their lab, and Eric Martens and lab for helpful discussions and sharing reagents. This work was supported by NIH grants DK095782 and DK091191 (G.N.), JSPS KAKENHI (22H03541), JST PRESTO (JPMJPR1537), AMED-CREST (JP23gm1010009), JST ERATO (JPMJER1902), and the Food Science Institute Foundation (S.F.). NIH F32DK118800 (J. M. P.). NIH K99AI159620 and R00AI159620 (G. C.-F.). NIH R03AI139557, R01AI136520, AFRI 2017-67015-26085, NIFA 59-6066-4-005, and NACA 58-6066-4-044 from USDA (S.P. and M.M.).

Author contributions

J.M.P. and G.N. conceived and designed all the experiments; J.M.P. performed all the experiments with help from G.C.-F. and R.C.; A.H. and S.F. performed the metabolome analysis; S.P. and M.M. created reagents and suggested experiments. N.I. performed bioinformatic analyses. J.M.P. and G.N. analyzed all the data and wrote the manuscript with contributions from all authors.

Competing interests

The authors declare no competing interests.

Additional information

Supplementary information The online version contains supplementary material available at <https://doi.org/10.1038/s41467-025-59706-1>.

Correspondence and requests for materials should be addressed to Gabriel Núñez.

Peer review information *Nature Communications* thanks Tyrrell Conway, Christopher Schubert and the other, anonymous, reviewer for their contribution to the peer review of this work. A peer review file is available.

Reprints and permissions information is available at <http://www.nature.com/reprints>

Publisher's note Springer Nature remains neutral with regard to jurisdictional claims in published maps and institutional affiliations.

Open Access This article is licensed under a Creative Commons Attribution-NonCommercial-NoDerivatives 4.0 International License, which permits any non-commercial use, sharing, distribution and reproduction in any medium or format, as long as you give appropriate credit to the original author(s) and the source, provide a link to the Creative Commons licence, and indicate if you modified the licensed material. You do not have permission under this licence to share adapted material derived from this article or parts of it. The images or other third party material in this article are included in the article's Creative Commons licence, unless indicated otherwise in a credit line to the material. If material is not included in the article's Creative Commons licence and your intended use is not permitted by statutory regulation or exceeds the permitted use, you will need to obtain permission directly from the copyright holder. To view a copy of this licence, visit <http://creativecommons.org/licenses/by-nc-nd/4.0/>.

© The Author(s) 2025